RF Noise Models of MOSFETs- A Review

S. Asgaran, and M. Jamal Deen

Electrical and Computer Engineering Department, CRL 226
McMaster University, Hamilton, ON L8S 4K1, Canada, jamal@mcmaster.ca

ABSTRACT

A thorough study of high frequency MOSFET noise compact modeling with emphasis on channel thermal noise modeling is presented. Although the modeling of MOSFET noise dates back to many years ago, the enhanced noise generated in short channel MOSFETs has made researchers revisit the problem to develop better models, especially in recent years. In this review, a detailed discussion of the most recent models published in the literature is provided. Each model is investigated in terms of physical and analytical aspects of the model, and some comments are made in each case. The induced gate noise, which is important in today's high frequency applications, is also briefly reviewed at the end of this paper.

Keywords: MOSFET, compact modeling, thermal noise

1 INTRODUCTION

The ever decreasing channel length of MOSFET has enabled circuit designers to design circuits that can operate at very high frequencies. An important application of these circuits can be found in wireless communications where most often the signal received by the receiver is so small that only a limited amount of noise can be tolerated in the system. Therefore, it is very important for circuit designers to be able to predict the noise of MOS devices with reasonable accuracy and also to understand the noise dependence on the geometrical and biasing conditions of the device. Thus, a simple and yet accurate compact noise model is called for.

Two types of noise are present in MOSFET in strong inversion at moderate frequencies: Flicker noise and thermal noise. Although, the effect of flicker noise at high frequencies is negligible, another type of noise, which is generated due to the capacitive coupling between the MOSFET channel and its gate, arises at very high frequencies and is called induced gate noise. Fig. 1 shows the contributions of different types of noise in MOSFET versus frequency [1].

The noise sources that generate thermal noise in MOSFET are the channel, S_{iD}, the actual resistances associated with the device electrodes, i.e. R_G, R_D, R_S, resistances between the substrate and source/drain, i.e. R_{DB}, R_{SB}, R_{DSB}, and the induced gate noise, S_{iG}.
Fig. 2 shows the equivalent compact circuit MOSFET model, including the noise sources, which is suitable for high frequency applications [2].

In this paper we present a comprehensive review of major channel thermal noise models reported hitherto in the literature, followed by a discussion on the induced gate noise and other noise sources in MOSFET.

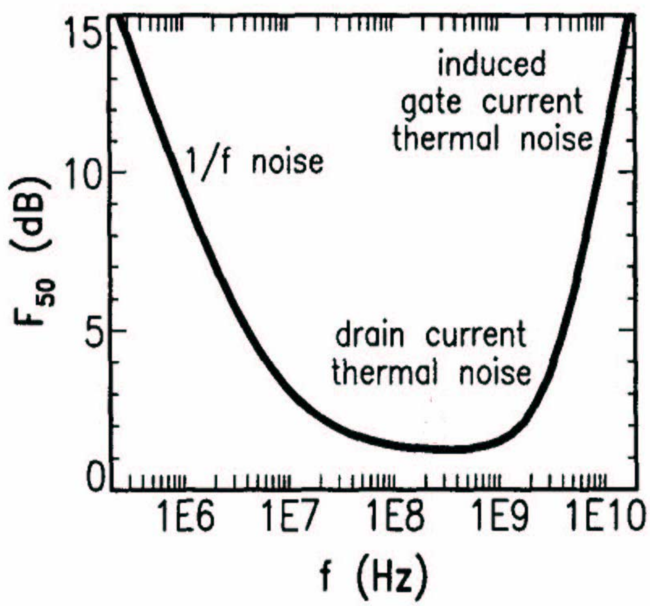

Fig. 1: Simulated 50-Ω noise figure versus frequency, for a 1000/0.25 (μm/μm) n-channel MOSFET [1].

2 MOSFET CHANNEL THERMAL NOISE

Modeling of the thermal noise generated in the MOSFET channel goes back to a few decades ago. The well-known Klaassen-Prins [3] model gives the MOSFET channel noise as

$$S_{iD} = \frac{4kT}{L^2 I_D} \int_0^{V_{DS}} g^2(V_0)dV_0 \,. \tag{1}$$

Here, k is the Boltzman constant, T is the device temperature, L is the MOSFET channel length, I_D is the drain current of the device, V_0 is the dc potential at point x along the channel with reference to the source electrode, and $g(V_0)$ is the channel conductance at point x. This model is obtained by calculating the current noise of small sections of the MOSFET channel and integrating the noise currents all over the channel. Van der Ziel [4] includes the so-called hot electron effects in the model by replacing the lattice temperature with carrier temperature, $T_e(x)$, and modified the model to

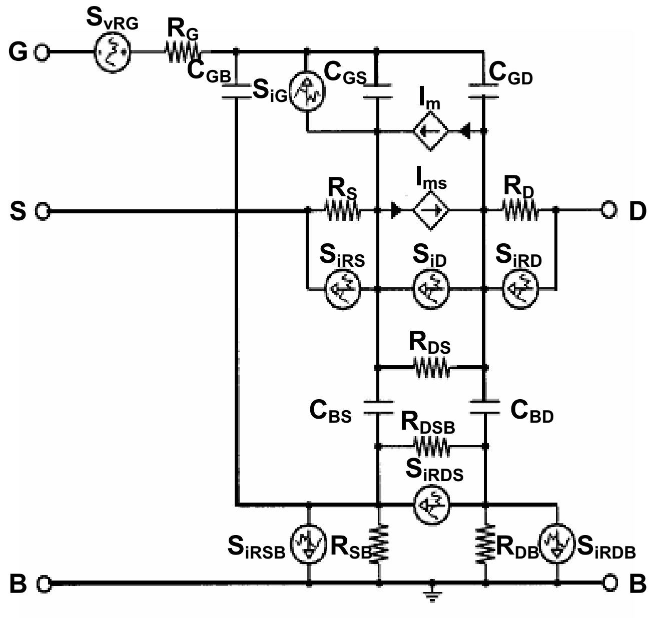

Fig.2: The equivalent compact circuit model of the MOSFET, which is suitable for high frequency applications [2].

$$S_{iD} = \frac{4kT}{L^2 I_D} \int_0^{V_{DS}} \frac{T_e(x)}{T} g^2(V_0) dV_0 \,. \tag{2}$$

It is assumed that the relation between these two temperatures can be described with a quadratic function as [4], [5]

$$T_e(x) = T\left\{1 + \delta\left[\frac{E(x)}{E_C}\right]^2\right\}, \tag{3}$$

where δ is an empirical constant, $E(x)$ is the longitudinal electric field along the channel, and E_C is the critical channel field beyond which the carriers are velocity saturated. It is experimentally shown in [5] that this relation is inadequate for the channel fields beyond E_C, and $T_e(x)$ dependence on $E(x)$ is better described by an exponential relation.

Using a similar approach, a rather simpler model is developed by Tsividis [6] as

$$S_{iD} = \frac{4kT\mu}{L^2} Q_{inv}\,, \tag{4}$$

where μ is the mobility of carriers in the channel and Q_{inv} is the total inversion layer charge.

The models presented in (1) and (4) are developed for long channel devices, where the carriers are in thermal equilibrium with the lattice. However, as the MOSFET channel becomes shorter, significant increase in the drain current noise is observed [7], as shown in Fig. 3

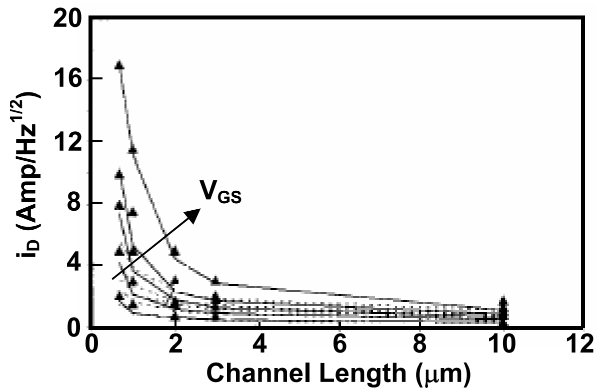

Fig.3: Channel thermal noise current of MOSFETs with different channel lengths, and different operating points (V_{GS}) [7].

In the past few years, several models have been developed to explain this enhanced noise. In these models, the MOSFET channel is divided into two sections as depicted in Fig. 4. The first section is called the linear region, where the gradual channel approximation (GCA) holds, i.e. the channel field is much smaller than the critical field. The second part is where the carriers travel at their saturation velocity. The difference between different models is the approach taken to model the noise of each of the two sections of the channel. The following is a review of major channel thermal noise models published recently.

3 CHANNEL THERMAL NOISE IN SHORT CHANNEL MOSFETS: A REVIEW

3.1 Model of Park et al.

The drain current noise spectral density of MOSFET is given in [8] as

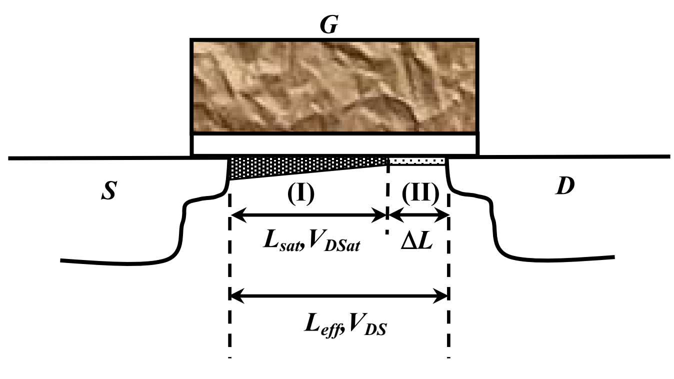

Fig. 4: Cross section of the channel of a MOSFET, divided into two regions: (I) gradual and (II) velocity saturation regions. L_{sat} is the point in the channel where the channel field $E(x)$ is equal to the critical field, E_c, and the velocity of carriers is equal to their saturation velocity, v_{sat}. ΔL is the length of the pinch-off or velocity saturated region.

$$S_{iD} = g_{DS}^2 \left\{ \frac{4kTV_c}{I_D} \left[\frac{\frac{\alpha^2}{3} V_C^2 - \alpha V_{GT} V_C + V_{GT}^2}{(V_{GT} - \alpha V_C)^2} + \delta \right] \times \cosh^2 (L_{sat}/l) + \frac{4qDI_D}{3\varepsilon_s^2 W^2 x_j^2 v_s^3} L_{sat}^3 \right\}. \quad (5)$$

Here, g_{DS} is the channel conductance, V_C is the channel potential at the point where $E(x)=E_C$, α is the bulk-charge effect, $V_{GT}=V_{GS}-V_{th}$ where V_{th} is the MOSFET threshold voltage, δ is the same as δ in (3), L_{sat} is the length of the pinch-off region of the channel in saturation and equal to $L_{sat}=l\sinh^{-1}((V_{DS}-V_C)/E_C l)$, where $l=(x_j t_{ox}\varepsilon_s/\varepsilon_{ox})^{1/2}$, D is the high field diffusion constant, W is the width of the device, x_j is the drain junction depth, q is the electron charge, and v_s is the saturated velocity of the dipole layer.

In this model, the voltage noise in the linear part of the channel is calculated using the simple drain current model provided by BSIM [9]. However, the mobility degradation effect due to the longitudinal electric field in this part of the channel is not taken into account, which in turn could result in reduced accuracy of the model, especially in very short channel devices. The carrier temperature, i.e. T_e in (3), is used in the linear part of the channel to account for hot electrons.

In this model, the noise in the velocity saturation part of the channel is believed to come from intrinsic diffusion noise sources in that region. The total drain current noise of MOSFET is the product of the channel conductance and the sum of noise voltages generated in the two sections of the channel. This way of calculating the total drain current noise is not correct simply because the MOSFET channel conductance is a function of the position along the channel and is not constant.

Moreover, this model has been verified experimentally by using the measured data presented by Abidi in [10], which may not be as reliable as recent measured noise data. This is because his noise measurements were carried out under very high V_{DS}, i.e. V_{DS}=4 V, and hence a significant part of the noise comes from avalanche noise, which is caused by drain to bulk current [11].

3.2 Model of Triantis et al. [12]

Similar to the model presented in [8], this model calculates the *voltage* noise generated in the two sections of the channel first and the total drain current noise is the product of the channel conductance and the total voltage noise of the channel. Carrier temperature is used in both the linear and velocity saturated parts of the channel, with different models used to model the temperature of the carriers.

In this model, it is assumed that the noise generated in the second part of the channel is thermal noise generated from small sections of Δx, located at point x, with resistance Δr_D, given by

$$\Delta r_D = \frac{E_{II}(x)\Delta x}{I_D} \quad (6)$$

where $E_{II}(x)$ is the longitudinal electric field at point x in the second part of the channel and I_D is the drain current. This way of modeling the noise is questionable because of the fact that Δr_D is an ac resistance and does not contribute any thermal noise.

To calculate the voltage fluctuations at the drain side of the channel, it is assumed that the electric field in the linear part of the channel is simply the voltage across this region divided by the length of the region. This assumption is not correct, especially in very short channel devices since in the linear part of the channel, the electric field is a nonlinear function of the position [13]. To experimentally verify the model, the measured data presented in [10] is used in [12].

3.3 Model of Knoblinger et al.

The channel noise of MOSFET is given in [14] in a closed-form as

$$S_{iD} = \frac{4kT}{L^2}\mu_{eff} Q_{inv} + \delta \frac{4kTI_D}{L^2 E_C^2} V_{DS} + \frac{4kTI_D}{L^2 E_C} \frac{2}{\alpha} \left\{ \arctan\left[\exp(\alpha \Delta L)\right] - \arctan(1) \right\} + \delta \frac{4kTI_D}{L^2 E_C} \frac{1}{\alpha} \sinh(\alpha \Delta L) \cdot \quad (7)$$

Here, μ_{eff} is the effective carrier mobility, ΔL is the length of the pinch-off region, α is the inverse of l, which is defined before, and the rest of the parameters are the same as before.

On the contrary to the previously mentioned models, this model calculates the *current* noise generated from each part of the channel by integrating the elemental thermal noise currents generated from small sections of the channel.

The hot electron effect is included in the model by using the carrier temperature, (3), in both parts of the channel with different models for the longitudinal electric field, $E(x)$. It is interesting to note that in this model, the carrier mobility is defined as $\mu(x)=v(x)/E(x)$ in both linear and saturation parts of the channel. This is of course not true because of the fact that the carriers are velocity saturated in the second part and using this relationship is not very meaningful.

3.4 Model of Scholten et al.

Based on the previously mentioned Klaassen-Prins model, the current noise spectral density of MOSFET is given in [1] as

$$S_{iD} = \frac{1}{L^2 I_D} \int_0^{V_{DSat}} 4kT_e(x) g^2(V) dV \quad (8)$$

where T_e is the temperature of the carriers, and $g(V)$ is given by

$$g(V) = W\mu Q_{inv}(V) \quad (9)$$

where V is the quasi-Fermi potential. The effect of velocity saturation on the carrier mobility is modeled by (10) as

$$\mu = \frac{\mu_{eff}}{\left[1 + \left(\frac{E}{E_C}\right)^p\right]^{1/p}} \quad (10)$$

where μ_{eff} is the effective mobility and p=1 and 2 for p-channel and n-channel MOSFETs, respectively [1].

The relation between T and T_e in this model is given as

$$T_e = T\left(1 + \frac{E}{E_C}\right)^n \quad (11)$$

where n is between 0 and 2. A comparison between measured and modeled channel thermal noise currents using the model in (8) is given in [1] and is shown in Fig. 5. It can be seen from Fig. 5, that the measured values are best modeled when there is no carrier heating, i.e. n=0. Therefore, introducing the carrier temperature [8], [12], [14], to model the channel thermal noise is questionable.

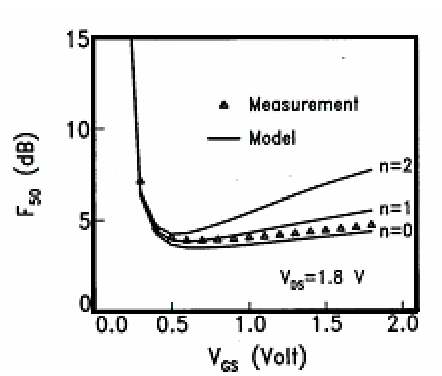

Fig. 5: Measured (symbols) and modeled (lines) 50-Ω noise figure of an NMOSFET with channel length L=0.18 µm versus the gate to source voltage, V_{GS} [1].

3.5 Model of Chen et al.

A simple model similar to the model presented in [6] is developed in [15] as

$$S_{iD} = \frac{4kT\mu_{eff}}{L_{elec}^2} Q_{inv} + \delta \frac{4kTI_D}{L_{elec}^2 E_C^2} V_{DSat} \,. \quad (12)$$

This model is based on the model in (4), with L replaced by L_{elec}, which is the electrical channel length of the MOSFET defined as L_{elec}=L_{eff}-ΔL, where L_{eff} is the effective channel length and ΔL is the length of the pinch-off region. The second term in (12) is added to account for the carrier heating effect. However, in experimental verification of (12), δ is set to 0, and very good agreement with the measured data is achieved [15]. This is in agreement with [1] that no carrier heating is needed to model the channel thermal noise.

To develop (12), the channel thermal noise generated from the first section of the channel is obtained by integrating the noise currents of small sections of the channel from the source side of the channel to L_{elec}. It is argued in [15] that the noise generated from the velocity saturated part of the channel is negligible. This is because in this part of the channel, the carriers do not respond to the local electric field fluctuations, caused by the voltage noise. This argument is experimentally verified in [15], where it is shown that the noise dependence on the drain to source voltage is negligible, as shown in Fig. 6.

3.6 Model of Scholten et al.

A revised version of the model given in (8) is presented in [16]. However, in agreement with [15] the electrical channel length is used instead of L, to include the channel length modulation effect. The velocity saturation effect is accounted for via the local channel conductance, $g(V)$ [16]. The noise contribution from the second part of the channel is neglected in this model following the argument made in [15].

A closed-form expression, based on (8), is given in [14] for the drain current noise spectral density, (eq. (24) in [16]).

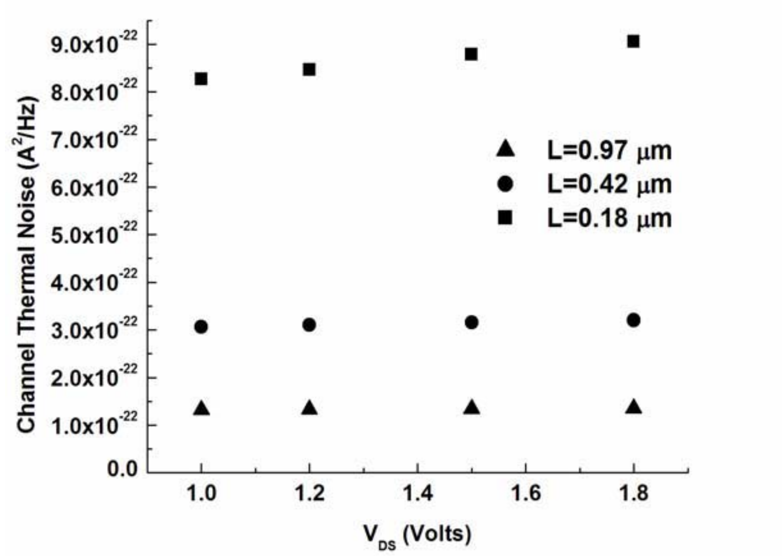

Fig. 6: Measured noise spectral density versus V_{DS} of n-type MOSFETs with channel width W=60 μm and channel lengths L=0.97, 0.42 and 0.18 μm, biased at V_{GS}=1 V. Measured noise data are from [15].

However, since this expression is a function of the channel surface potential, it is not suitable for fast calculation and does not show the explicit dependence of the noise current on the biasing conditions of the MOSFET.

In addition, the experimental data given in [16] show that the model presented in [6] cannot accurately predict the noise of deep-submicron devices at relatively high gate to source voltages, as shown in Fig. 7. This may be due to the approximations made to calculate the channel conductance, *g(V)*.

4 INDUCED GATE NOISE

The MOSFET channel acts as a distributed RC network at high frequencies [4]. The capacitive coupling to the gate represents the distributed capacitance and the MOSFET channel represents the distributed resistance. Therefore, the voltage fluctuation in the MOSFET's channel is coupled to its gate, causing the induced gate noise current to flow. This noise is modeled by a current source connected in parallel with C_{gs} (see Fig. 2). Unlike channel thermal noise, the power spectral density of induced gate noise is dependent on the frequency of operation an is given as [2]

$$S_{iG} = 4kT\delta \frac{\omega^2 C_{gs}}{5g_{ms}} \tag{13}$$

where g_{ms} is the source transconductance, and δ is a bias dependent factor equal to 4/3 in long channel devices.

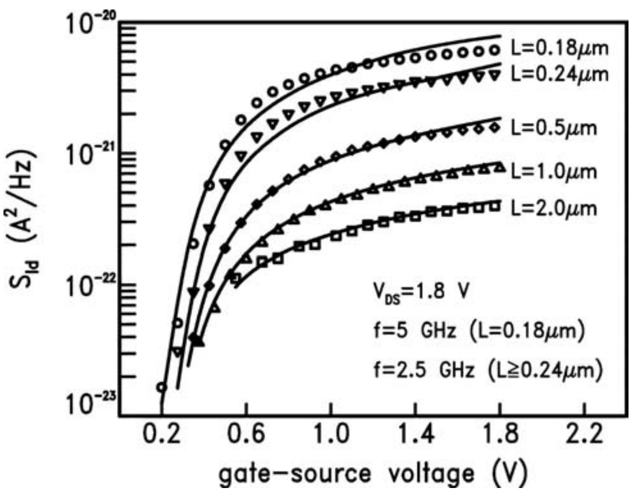

Fig. 7: Measured (symbols) and modeled (lines) drain current noise spectral density of MOS devices with different channel lengths versus V_{GS}. The drain to source voltage is fixed at 1.8 V [16].

Since the channel thermal noise and induced gate noise have the same origin, they are correlated with a correlation factor *c*, which is equal to *j0.395* in long channel devices, and slightly smaller (between *j0.35* to *j0.3*) in short channel devices [17].

The induced gate noise, S_{iG}, and the correlation noise, $\overline{i_g i_d^*}$, of NMOSFETs with different channel length versus frequency are shown in Figs. 8 and 9, respectively [18]. It has been found that the induced gate noise and the correlation noise are proportional to f^2 and f, respectively.

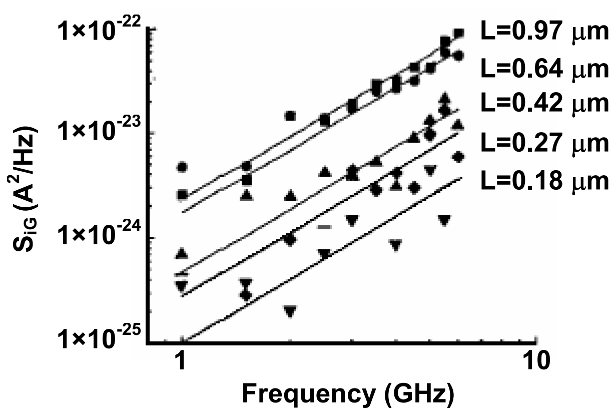

Fig. 8: Induced gate noise of NMOSFETs with different channel length biased at V_{DS}=1 and V_{GS}=1.2 V, versus frequency [18].

It can also be seen from Figs. 8 and 9 that both noises decrease with decreasing the channel length because of the reduction in the gate to source capacitance, C_{gs}.

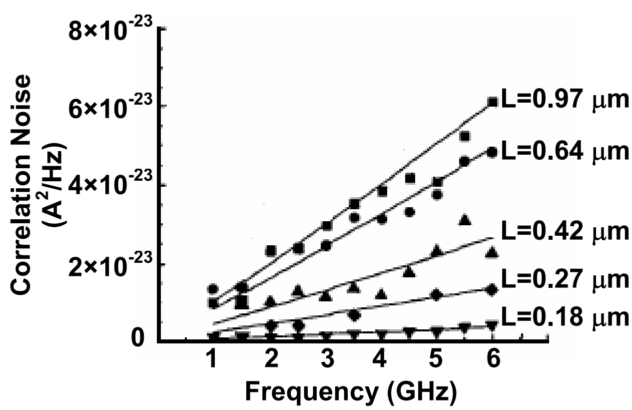

Fig. 9: Correlation noise, $\overline{i_g i_d^*}$, of NMOSFETs with different channel length biased at V_{DS}=1 and V_{GS}=1.2 V, versus frequency [18].

The dependence of the induced gate noise on V_{GS} and V_{DS}, is shown in Figs. 10 and 11, respectively [16].

5 THERMAL NOISE FROM PARASITIC RESISTANCES

As mentioned before, four types of resistance exist in a MOSFET: gate resistance, source and drain resistance, and the resistance between substrate and source/drain electrodes (see Fig.2). The gate resistance has a strong impact on the maximum oscillation frequency of the MOSFET, and the source/drain resistances have an impact on the current drive capability of the MOSFET [19]. The thermal noise associated with these resistances can be easily expressed as

$$S_{iD} = 4kT/R \tag{14}$$

where R is the value of each resistance, which depends on the extraction method used. It should be noted that different extraction techniques yield slightly different values [19].

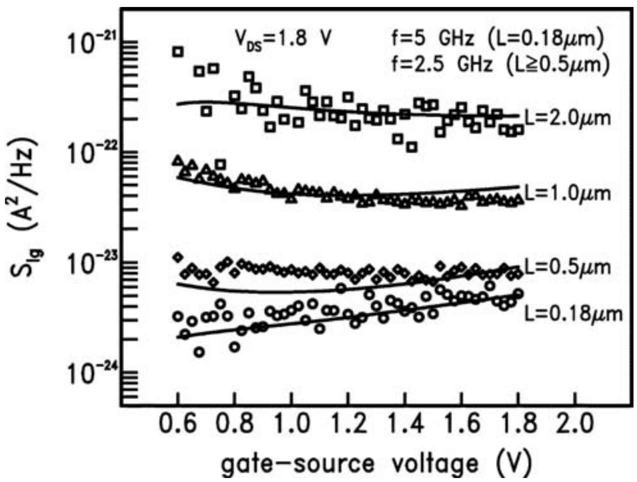

Fig.10: Induced gate noise of MOSFETs with different channel length versus the gate to source voltage V_{GS} [16].

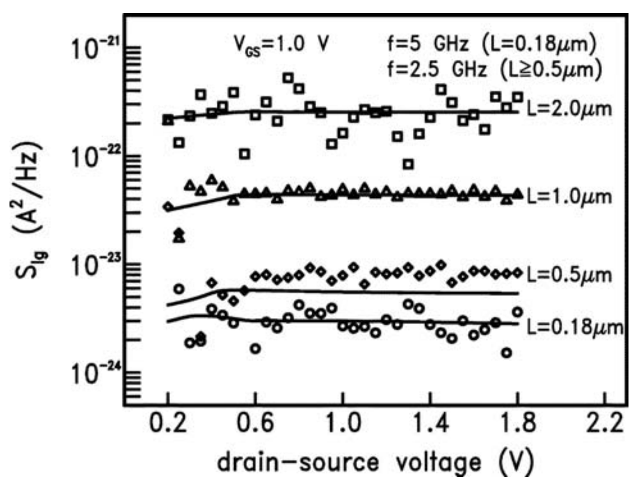

Fig.11: Induced gate noise of MOSFETs with different channel length versus the drain to source voltage V_{DS} [16].

6 CONCLUSIONS

A review of the MOSFET high frequency thermal noise modeling, with emphasis on channel thermal noise, is presented. Several channel noise models are reviewed and discussed in detail. The models are common in the fact that they divide the MOSFET channel into two sections of linear and velocity saturation. However, each model has its own approach of modeling the noise in each part of the channel. Most of these models use a carrier temperature, which is a function of the lattice temperature to model the hot electron effects. However, it is shown that there is no need to include the carrier temperature to model the noise. In addition, the induced gate noise modeling, which is important at high frequencies, is briefly reviewed together with the noise generated from parasitic resistances of MOSFET.

Since the demand for low power circuit design is increasing everyday, the operating region of MOSFET is being pushed to weak and moderate inversion. However, there has been little published data on MOSFET noise modeling in these regions of operation especially at high frequencies. Therefore, in the near future, analytical noise models that are valid in moderate and weak inversion regions of operation will be required.

REFERENCES

[1] A. J. Scholten et al. *IEDM* 1999, pp. 155-158.
[2] C. Enz, *IEEE Trans. Microwave Theory Tech.*, vol. 50, no. 1, Jan. 2002.
[3] F. M. Klaassen, and J. Prins, “Thermal noise of MOS transistors,” *Philips Res. Reps.*, vol. 22, pp. 504-514, 1967.
[4] A. van der Ziel, *Noise in Solid State Devices and Circuits*. New York: Wiley, 1986.
[5] D. Gasquet, Ph.D. thesis, Universite de Montpellier II. P. Glinelli et al., “Noise temperature and hot carrier thermal conductivity in semiconductors,” in second *ELEN Workshop*, Grenoble, France, 1995.
[6] Y. P. Tsividis, *Operation and Modeling of the MOS transistor*. New York: Wiley, 1987.
[7] P. Klein, *IEEE Electron Dev. Letters*, vol. 20, no. 8, pp. 399-401, Aug. 1998.
[8] C. H. Park, and Y. J. Park, *Solid State Elctronics*, vol. 44, pp. 2053-2057, 2000.
[9] B. J. Sheu, D. L. Scharfetter, P-K. Ko, and M-C. Jeng, *IEEE J. Solid-State Circuits*, vol. sc-22, pp.558-566, Aug. 1987.
[10] A. Abidi, *IEEE Trans. Electron Devices*, ED-33, no. 11, NOV. 1986.
[11] A. J. Scholten et al. *IEDM* 1999, pp. 129-132.
[12] D. P. Triantis, A. N. Birbas, and D. Kondis, *IEEE Trans. Electron Devices*, vol. 43, no. 11, pp.1950-1955, Nov. 1996.
[13] K. Takeuchi, and M. Fukuma, *IEEE J. Solid-State Circuits*, vol. 41, pp. 1623-1627, Sep. 1994.
[14] G. Knoblinger, P. Klein, and M. Tiebout, *IEEE J. Solid-State Circuits*, vol. 36, pp. 831-837, May 2001.
[15] C. H. Chen and M. J. Deen, *IEEE Trans. Electron Devices*, vol. 49, pp. 1484-1487, Aug. 2002.
[16] A. J. Scholten, L. F. Tiemeijer, R. van Langevelde, R. J. Havens, A. T. A. Zegeres-van Duijnhoven, and V. C. Venezia, *IEEE Trans. Electron Devices*, vol. 50, pp. 1-15, Mar. 2003.
[17] T. Manku, *IEEE J.Solid-State Circuits,* vol. 34, pp. 277–285, Mar. 1999.
[18] M. J. Deen, and C. H. Chen, *IEEE Custom Integrated Circuits Conference,* pp. 201-208, May 2002.
[19] C. H. Chen, and M. J. Deen, *Solid-State Electronics*, vol. 42, no. 11, pp. 2069-2081, 1998.